International Journal of Biological Macromolecules 213 (2022) 486–497

Contents lists available at ScienceDirect

International Journal of Biological Macromolecules

journal homepage: www.elsevier.com/locate/ijbiomac

Production of chitosan-based biodegradable active films using bio-waste enriched with polyphenol propolis extract envisaging food packaging applications

Cristiane De Carli [a,b], Volkan Aylanc [a], Kheira M. Mouffok [a], Arantzazu Santamaria-Echart [a], Filomena Barreiro [a], Andreia Tomás [a], Celeide Pereira [b], Paula Rodrigues [a], Miguel Vilas-Boas [a,*], Soraia I. Falcão [a,*]

[a] Centro de Investigação de Montanha (CIMO), Instituto Politécnico de Bragança, Campus de Santa Apolónia, 5300-253 Bragança, Portugal
[b] Universidade Tecnológica Federal do Paraná – UTFPR, Campus Medianeira, 85884-000 Medianeira, Brazil

ARTICLE INFO

Keywords:
Active chitosan film
Crayfish
Propolis extract
Antioxidant
Antimicrobial
Biodegradable film
Food packaging

ABSTRACT

Developing biodegradable active films has been a promising green approach to overcoming global concerns over the environmental pollution and human health caused by plastic utilization. This study aimed to develop active films based on chitosan (CS), produced from waste crayfish (*Procambarus clarkii*) shells enriched with bioactive extract (5–20%) of propolis (PS) and to characterize its properties, envisaging food packaging applications. The chromatographic profile of PS extract confirmed its richness, with 41 phenolic compounds. With increasing extract addition to the chitosan, the thickness of the films increased from 61.7 to 71.7 μm, causing a reduction in the light transmission rate, along with a greenish colour shift. The interactions between PS extract and CS was confirmed by infrared spectroscopy, at the same time that the microstructural integrity of the films was checked on the scanning electron microscopy micrographs. The findings also showed that addition of PS enhanced the films thermal stability and mechanical properties e.g., tensile modulus, yield strength, and stress at break. Besides, it improved the antioxidant and antimicrobial activities. Overall, CS-based composite films seem a promising green alternative to petroleum-based synthetic plastics allowing to extend the shelf life of food products due to their eco-friendly nature.

1. Introduction

The generation of large amounts of waste as a consequence of the intensive use of petroleum-based plastics by the food industry has raised the concerns of society and, particularly, the scientific community. These wastes, which are formed as a result of food packaging and distribution, cause serious environmental pollution owing to non-biodegradability [1]. Biopolymer-based packaging materials have been devoted to considerable attention as a green alternative to replacing synthetic plastics towards a sustainable environment [2–4]. The use of various natural polymeric materials such as polysaccharides, proteins, and lipids in active food packaging may help to meet this need, especially those that are recovered from industrial wastes and underused sources [3,5]. Active films prepared from such sources are biodegradable, which combined with their antioxidant and antimicrobial activities, makes them as good candidates for both extending the shelf-life and increasing the quality of food products [6].

Among biopolymers, active films based on chitosan (poly-β-(1–4)-*N*-acetyl-D-glucosamine), which is obtained from the deacetylation of chitin, is a promising candidate with a broad range of applications in many fields such as food, pharmaceuticals, agriculture, and cosmetics, directly or indirectly, due to its biocompatible, non-toxic, biodegradable and excellent film-forming properties [6–8]. However, in opposition to these favourable properties of CS-based films, they have some disadvantages, including low UV light barrier and limited mechanical properties. Along with this, their inherent hydrophilic nature makes CS films highly sensitive to moisture, which is another considerable drawback for packaging products with high water activity/content [2]. Thus, natural bioactive agents such as phenolic compounds, essential oils, and plant extracts, or nanocrystals and nanofibers from biopolymers are

* Corresponding authors.
E-mail addresses: mvboas@ipb.pt (M. Vilas-Boas), sfalcao@ipb.pt (S.I. Falcão).

https://doi.org/10.1016/j.ijbiomac.2022.05.155
Received 30 January 2022; Received in revised form 10 May 2022; Accepted 22 May 2022
Available online 29 May 2022

commonly explored to overcome such obstacles and strengthen the physical and mechanical properties of CS films, but also to their biological activity [9–15].

Even though CS has inherent antioxidant and antimicrobial activity, it may not always be at a level to prevent intense microbial growth and oxidation in the ambient and therefore the adding of natural antioxidant and antimicrobial compounds to provide a high level of food safety and quality allows the development of active packaging based on a sustainable approach [2]. In this regard, PS or bee glue is a potent source of natural bioactive compounds to be incorporated into biopolymeric matrices [4,16]. PS is a chemical weapon of bees against pathogenic microorganisms and diseases and is used for the continuous maintenance of a healthy hive. It is a resinous substance collected by foragers bees from buds and plant exudates, that is mixed with secretions from their glands [17]. Over 300 volatile and non-volatile components have been specified in PS around the world [18]. In accordance with the literature, although the different PSs demonstrate a broad variety of chemical compounds, phenolics represent the predominant family [18,19]. Additionally, it has been confirmed that phenolic compounds, together with terpenoids play an important role in the biological activity of PS [20,21]. These characteristics make PS a suitable natural source for exploitation in active film production.

Previous studies have demonstrated that the addition of PS, as a natural agent, into polymers such as starch, gelatine, carrageenan, CS, polypropylene, and ethylene vinyl alcohol increased the physicochemical properties and biological activities of the films [4,16,22–24]. However, there are quite limited studies reporting the characterization and biological properties of CS films enriched with PS.

Thus, this study aimed to produce biodegradable composite films based on CS obtained from waste crayfish shells and reinforced with PS extract at different ratios. The produced films were characterized either for the physicochemical (colour, thickness, optical transmittance, Fourier transform infrared (FT-IR) spectroscopy, thermogravimetric analysis (TGA), scanning electron microscopy (SEM), mechanical properties, degradability in nature) and biological properties (antioxidant, anti-bacterial, anti-fungi, and anti-mould activity).

2. Materials and methods

2.1. Chemicals and reagents

Ethanol (absolute, ≥99.8%), acetonitrile (HPLC grade, ≥99.9%), hydrochloric acid (analytical reagent grade), sodium hydroxide (analytical reagent grade), chloroform (analytical reagent grade), methanol (HPLC grade, ≥99.8%), acetic acid (analytical reagent grade) and potassium persulfate (ACS grade, 99+%) were purchased from Fisher Scientific (Pittsburgh, PA, USA). Glycerol, 2,2-diphenyl-1-picrylhydrazyl (DPPH), 2,2′-azino-di-(3-ethylbenzthiazoline sulfonic acid) (ABTS), caffeic acid, *p*-coumaric acid, kaempferol, pinocembrin and chrysin were purchased from Sigma-Aldrich (St. Louis, MO, USA), and all of them were of analytical grade. Purified water, treated in a Milli-Q water purification system (TGI pure system, Houston, TX, USA), was used in all the experiments.

2.2. Sample collection and preparation

The propolis sample (from *Apis mellifera* hives) was obtained from local beekeepers at Bragança, Northeast of Portugal, in 2020, and corresponds to typical poplar type from temperate regions. The crayfish (*Procambarus clarkii*), which is an invasive species in Portuguese freshwaters, were collected in the river (Fervença river) in Bragança, Portugal in September 2020.

2.3. Preparation of propolis extract

The PS extract was obtained by a hydro-ethanolic extraction procedure [21]. Briefly, 20 mL of 80% ethanol/water was mixed with 2 g of PS and kept at 70 °C, at 65g for 1 h. The mixture was then filtered through the Whatman No 4. filter paper and the residue was re-extracted under the same conditions. After combining the extracts, the solvent was evaporated in a rotary evaporator (model Hei-VAP from Heidolph, Schwabach, Germany) at 40 °C. In the last step, the PS extract was freeze-dried using a lyophilizer (FreeZone 4.5 model 7750031 from Labconco, Kansas City, KS, USA) and stored at room temperature until further analysis.

2.4. LC/DAD/ESI-MS^n phenolic compounds analysis

For the analysis, PS extract (20 mg) was dissolved in 2 mL of 80% ethanol/water. The solution was filtered through a 0.22 μm membrane and kept in the freezer at −20 °C, until analysis.

A Dionex UltiMate 3000 ultra-pressure liquid chromatography instrument connected to a diode array and attached to a mass detector was used for LC/DAD/ESI-MS^n analyses (Thermo Fisher Scientific, San Jose, CA, USA). LC was run in a Macherey-Nagel Nucleosil C18 column (250 mm × 4 mm id; particles diameter of 5 mm, end-capped) and the temperature was kept constant at 30 °C. The conditions applied in the liquid chromatography were based on previous work [25]; the flow rate was 1 $mL{\cdot}min^{-1}$, and the injection volume was 10 μL. The final spectra data were accumulated in the wavelength interval of 190–600 nm, (see Supplementary material for the conditions of LC/DAD/ESI-MS^n analysis). Quantification was achieved using calibration curves for caffeic acid (0.0187–0.4 $mg{\cdot}mL^{-1}$; $y = 6.0 \times 10^7x - 26{,}360$; $R^2 = 0.996$), *p*-coumaric acid (0.0187–0.5 $mg{\cdot}mL^{-1}$; $y = 9.0 \times 10^6x - 35{,}105$; $R^2 = 0.999$), kaempferol (0.075–1.6 $mg{\cdot}mL^{-1}$; $y = 1.0 \times 10^6x - 58{,}666$; $R^2 = 0.997$), pinocembrin (0.0375–0.8 $mg{\cdot}mL^{-1}$; $y = 2.0 \times 10^6x - 52{,}498$; $R^2 = 0.997$), and chrysin (0.0375–0.8 $mg{\cdot}mL^{-1}$; $y = 4.0 \times 10^6x - 18{,}959$; $R^2 = 0.999$). When the standard was not available, the compounds were quantified using the calibration curve of the structurally closest standard, and the final result was given in equivalent terms, expressed as $mg{\cdot}g^{-1}$ of PS extract. The analysis was performed in triplicate.

2.5. Chitin isolation and chitosan production

Isolation of chitin and production of CS were performed according to the procedure outlined by Duman et al. [26]. Accordingly, after washing the crayfish shells with deionized water, the samples were dried at room temperature and ground in a mortar. In the first step, which was the demineralization process, 20 g of the sample was refluxed with 2 M HCl at 100 °C for 4 h. Afterwards, the samples were refluxed with 2 M NaOH for 18 h at 100 °C to obtain protein-free samples. In the final step, the samples were exposed to a mixture of deionized water, methanol and chloroform in a ratio of 4:2:1 for 2 h, at room temperature, to remove oil and pigments. The samples were then dried in the oven at 40 °C, for 72 h, to obtain chitin. After each of these steps, the samples were washed with deionized water at neutral pH (pH = 7.0).

To obtain pure CS, 3 g of dried chitin was refluxed with 60% NaOH at 100 °C for 4 h and then washed with deionized water to neutral pH. Finally, the CS was dried in the oven at 40 °C, for 48 h. Chitin isolation and CS production were performed in triplicate to determine the % of chitin content and CS productivity from this chitin source.

2.6. Films preparation

Film production was carried out according to Kaya et al. [11] with some minor modifications. Four different film-forming/coating solutions were prepared to contain 0% (w/w), 5% (w/w), 10% (w/w) and 20% (w/w) of PS extract by weight of CS. CS control film, without PS extract, was coded as CS-C, while films containing 5%, 10% and 20% of PS extract were coded as CS-PS5, CS-PS10 and CS-PS20, respectively. Briefly, 2 g of CS was dissolved in 100 mL of acetic acid solution (1% v/

v), with stirring (500*g*) for 24 h. Then, 1 mL of PS extract, prepared in 80% ethanol/water and glycerol (30% w/w of CS), were added to the film-forming solution. The solution was mixed using a homogenizer (Heidolph, Silent Crusher M, Schwabach, Germany) at 26,000*g* for 15 min and then subjected to ultrasonic treatment (J.P. Selecta, Barcelona, Spain) for 10 min, to remove air bubbles. A total of 20 mL of solution was poured onto a Petri dish (11 cm diameter) and left to dry at 25 °C and 50% relative humidity, at a drying oven (Memmert UNE400, Schwabach, Germany) for 48 h.

2.7. Physicochemical properties of films

2.7.1. Appearance and thickness measurement

The thickness of the produced films was measured with a digital micrometer (Mitutoyo, Kanagawa, Japan), and calculated using the average of nine measurements taken in different parts of the films.

2.7.2. UV–Vis light transmittance and colour

The UV–Vis light transmittance of films (2 × 2 cm) was measured from 400 to 700 nm using a spectrophotometer (V-730 UV–visible Spectrophotometer, Tokyo, Japan) [11].

The colour of the samples was analysed with a portable colourimeter CR400 from Konica Minolta (Chiyoda, Tokyo, Japan), at three different points, using film sections with 3 × 3 cm dimensions. The samples were evaluated using the CIELAB colour scale: $L^* = 0$ (black) to $L^* = 100$ (white); $-a^*$ (greenness) to $+a^*$ (redness); and $-b^*$ (blueness) to $+b^*$ (yellowness). The colourimeter was calibrated using a standard white plate as a blank. The colour difference (ΔE^*) was calculated according to the following Eq. (1) [27]:

$$\Delta E^* = \sqrt{\left(L^*_{standart} - L^*_{sample}\right)^2 + \left(a^*_{standart} - a^*_{sample}\right)^2 + \left(b^*_{standart} - b^*_{sample}\right)^2} \quad (1)$$

2.7.3. Fourier transform infrared (FT-IR) spectroscopy

FT-IR spectra were recorded for pure CS, PS extract, and for the films, using an FTIR (model: MB3000, ABB Inc., Quebec, Canada) equipped with attenuated total reflection (ATR) [11]. Spectra range was fixed between 4000 and 600 cm^{-1} with a resolution of 8 cm^{-1}. Spectra were processed using Horizon MB v.3.4 software (Cologne, Germany). The degree of deacetylation (DD) was calculated using Baxter's Eq. (2) [28]:

$$DD = 100 - \left(\frac{A_{1655}}{A_{3450}} \times \frac{100}{1.33}\right) \quad (2)$$

where A_{1655} and A_{3450} correspond to the area of the peaks centred at 1655 and 3450 cm^{-1}, respectively.

2.7.4. Thermogravimetric analysis (TGA)

Thermal stability of CS, PS extract, and for the films were analysed using a NETZSCH - TG 209 F3 Tarsus (Netzsch, Selb, Germany) thermogravimetric analyser equipment [29]. The samples were heated from 30 to 700 °C in a nitrogen atmosphere (40 mL·min^{-1}) at a scanning rate of 10 °C·min^{-1}. Thermogravimetric (TG) and derivative curves (DTG) were obtained using Netzsch Proteus thermal analysis (v.5.2.1) software.

2.7.5. Scanning electron microscopy

The surface morphology of the films was examined by scanning electron microscopy, using a Phenom Pro SEM system (Phenom, Eindhoven, Netherlands) with 15 kV and magnification range 160–350,000×.

2.7.6. Mechanical properties

The mechanical properties of the films were analysed using a mechanical tensile tester (Shimadzu Autograph AGS-X Series, Kyoto, Japan) equipped with a 10 kN load cell and pneumatic clamps to fix the samples. For each sample, 5 replicates of 20 mm × 30 mm dimensions were tested and a crosshead speed of 5 mm·min^{-1}. Tensile modulus, yield strength, stress at break, and strain at break of the films were determined from stress-strain curves of five specimens of each series.

2.7.7. Biodegradability

The biodegradation of CS-C and CS-PS composite films was tested with two different methods: water solubility and soil degradation.

The water solubility of the produced films was determined gravimetrically at 24 ± 1 °C according to a previously reported method, with minor modifications [11]. After drying the films to constant weight in the oven at 50 °C, they were cut into 2 × 3 cm pieces and incubated, for 48 h, in Petri dishes containing 30 mL of deionized water. Then, the film samples were retrieved and dried at 50 °C for additional 24 h. The dried film samples were weighed, and the weight loss % calculated according to Eq. (3):

$$\%WL = \left(\frac{W_i - W_f}{W_i}\right) \times 100 \quad (3)$$

where WL is the weight loss, W_i the initial weight and W_f the final weight of the samples.

The soil degradation of the CS-C and CS-PS films was performed according to the method specified by Kaya et al. [11]. Briefly, different plastic containers were filled with soil (organic matter content: 50%; pH: 6.0–7.0; conductivity: 40–80 μS·cm^{-1}; bulk density: 520 kg·cm^{-3}) for each tested film sample. Then, the dried films (2 × 3 cm) were buried at 5 cm below the surface of the soil and incubated at 25 ± 1.0 °C for 15 days. 10 mL of water was added to the samples daily to keep the soil moisture at 40%. After 15 days of incubation, the samples were retrieved from the soil, dried in an oven at 50 °C, and weighed. The soil degradation of the samples was calculated using Eq. (3). All tests were performed in triplicate.

2.8. Biological properties of films

2.8.1. Antioxidant activity

Antioxidant capacities of CS-C and CS-PS films were measured by DPPH and ABTS radical scavenging activity assays.

DPPH radical scavenging activity of the films was determined according to Aylanc et al. [29]. The film samples (10 mg), cut into small pieces (<4.0 mm), were placed in test tubes, mixed with 1 mL of DPPH solution (concentration: 6×10^{-5} M) and incubated in the dark, at room temperature, for 30 min. After this period, the absorbance was measured at 517 nm using a UV–Vis spectrophotometer (Centurion K2R series, Chichester, UK). The results were given as a percentage using Eq. (4):

$$Inhibition\ (\%) = \left(\frac{A_{control} - A_{sample}}{A_{control}}\right) \times 100 \quad (4)$$

where $A_{control}$ is the absorbance of DPPH solution while A_{sample} is the absorbance of film sample with DPPH. All tests were performed in triplicate.

The ABTS assay was performed by modification of the method previously reported [30]. Briefly, the ABTS stock solution was prepared by reacting ABTS (7 mM in deionized water) with 2.45 mM potassium persulfate. The mixture was left at room temperature for 16 h in the dark until it reached a stable oxidative state. ABTS working solution was prepared by diluting with ethanol to give an absorbance of 0.70 ± 0.05 at 734 nm. 1 mL of the working solution was mixed with 10 mg of the film sample and then incubated in a dark room, at room temperature, for 10 min. The absorbance of the samples was measured using a UV–Vis spectrophotometer (Centurion K2R series, Chichester, UK) at 734 nm. The results were given as a percentage using Eq. (4). All tests were performed in triplicate.

2.8.2. Antimicrobial activity

The antimicrobial activity of the composite films was evaluated against different microorganisms: bacteria: *Staphylococcus hominis* (*S. hominis*), *Pantoea* sp., *Arthrobacter* sp., *Erwinia* sp., *Bacillus cereus* (*B. cereus*), *Escherichia coli* (*E. coli*) and *Staphylococcus aureus* (*S. aureus*); yeast: *Metschnikowia rancensis* (*M. rancensis*); and moulds: *Cladosporium* sp., *Penicillium brevicompactum* (*P. brevicompactum*), *Botrytis cinerea* (*B. cinerea*) and *Alternaria* sp. (see Supplementary material Table S1 for microorganisms references).

The antimicrobial activities on food and human pathogen microorganisms of the CS-C and CS-PS films were determined using the agar drop diffusion method, according to the previously described procedure [31]. Briefly, agar plates were surface-inoculated with the microorganisms by homogeneously spreading the cell suspension with a swab, and then 50 μL of each film solution was loaded directly onto the agar. The tests were performed on a 12 × 12 cm plastic plates containing the culture media indicated in Table S2, depending on the type of microorganisms. Beside the films containing 0%, 5%, 10% and 20% PS extract, the commercial fungicide Teldor® (Bayer CropScience, Germany) and the antibiotic ampicillin sodium salt were also used as positive controls against fungi and bacteria, respectively, with a concentration of 1.5 mg·100 mL^{-1}. A solution of glycerol, ethanol and acetic acid (constituents of films) was applied as a negative control. The plates were incubated under the conditions described in Table S2. All tests were performed in triplicate.

2.9. Statistical analysis

All results were subjected to statistical analysis and denoted as mean ± standard deviation (SD). The data were analysed using GraphPad Prism version 8 (San Diego, CA, USA). One-way analysis of variance, followed by Tukey's multiple comparison test, was conducted to see whether there is a statistical significance. $p < 0.05$ was considered as significant.

3. Results and discussion

3.1. Polyphenolic compounds profile of propolis

Polyphenolic compounds in PS extract were evaluated by LC/DAD/ESI-MS^n. The chromatogram allowed the identification and quantification of a total of 41 compounds, with the results given in Fig. 1 and Table S3. The identification was done by comparing the fragmentation in MS^n spectra and the spectral information from UV in negative ion mode, with those available in the literature. Compounds such as caffeic acid (*m/z* 179), *p*-coumaric acid (*m/z* 163) and isoferulic acid (*m/z* 193) were the main phenolic acids present in the PS extract, while quercetin (*m/z* 301), pinocembrin (*m/z* 255), chrysin (*m/z* 253), galangin (*m/z* 269), pinobanksin (*m/z* 271) and its derivatives were the main flavonoids. PS from temperate zones including Portugal is generally of the poplar type [18], being the phenolic profile of PS sample in accordance with this PS type [17,32].

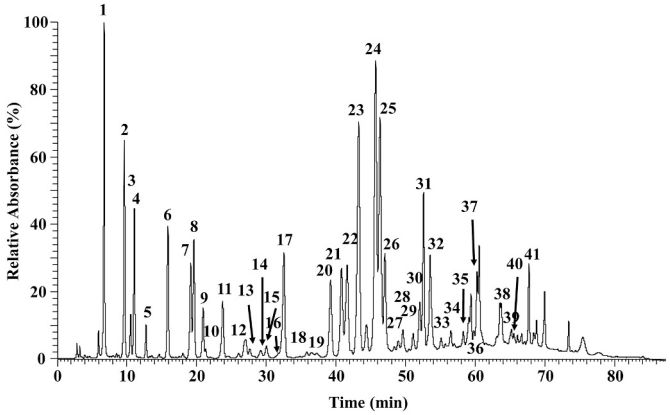

Fig. 1. Chromatographic profile of PS extract.

The flavonoids provided the largest quantitative contribution to the total phenolic composition of PS, and this was significantly ($p < 0.05$) higher than that of the phenolic acids. Pinocembrin was the major compound with a concentration value of 92.6 ± 0.0 mg·g^{-1}, followed by pinobanksin 3-*O*-acetate, galangin and quercetin with values of 89.4 ± 2.0 mg·g^{-1}, 69.4 ± 2.1 mg·g^{-1} and 57.0 ± 0.3 mg·g^{-1}. The findings reported by Woźniak et al. [33] and Souza et al. [34] indicate that the high phenolic compounds content of PS extracts effectively reflects their biological properties like high antioxidant and antimicrobial. Indeed, it is well known that high concentrations of phenolic substances or the presence of certain specific compounds, such as quercetin, show strong biological activities [18,21,35]. E.g., Pobiega et al. [36] attributed the biological action of pullulan coating containing ethanolic PS extract to the presence of high concentrations of phenolic acids and flavonoids such as cinnamic acid, chrysin, pinocembrin, quercetin and galangin.

3.2. Chitin content and chitosan yield

The chitosan yield of the complete procedure was recorded as 16%, corresponding to a chitin isolation from dry crayfish shells of 19%, and chitosan productivity from chitin of 83%. In previous studies, it was reported that the values of isolated chitin may range from 3 to 28% when using dry shells or different body parts of *Euphausia superba*, *Rhinolophus hipposideros*, *Catharsius molossus*, *Penaeus monodon*, *Schistocerca gregaria*, *Apis mellifera* and *Calosoma rugosa*, while the productivity of chitosan from chitin was estimated around 72–79% [37–40]. In a study conducted by Abdou et al. [41], the chitin content of crayfish was found to be 20%, which is in agreement with the obtained results.

3.3. Thickness, appearance, light transmission and colour of films

The thickness, colour, and light transmittance properties of the biopolymer-based films are parameters of considerable influence in food packaging and coating applications since they can positively or negatively affect both the quality of the applied food and consumer decisions. The appearance and thickness of CS-C and CS-PS films are shown in Figs. 2 and 3A, respectively. The overall appearance of the CS-C film was transparent with a thickness of 61.7 ± 9.8 μm. The inclusion of different proportions of PS extract (5%, 10% and 20%) showed a progressive increase in their thickness: 66.7 ± 8.2 μm, 70.0 ± 8.9 μm and 71.7 ± 7.5 μm, respectively, but with no statistically significant difference ($p < 0.05$) among them. This behaviour was observed also with the addition of *Berberis crataegina*'s fruit extract and seed oil to the CS film, increasing the film thickness from 45.4 ± 30.5 μm (control) to 99.2 ± 9.7 μm (fruit extract) and 84.8 ± 3.1 μm (seed oil) [12], and may be associated with different crosslinks established between the CS and the extracts.

Exposure of packaged food products to UV–vis light can cause an easily oxidative deterioration, undesirable colour change, and flavour. The optical transmittance of the films was measured in the visible light spectrum, Fig. 3B. The film transparency decreased with the addition of PS extract to the CS film matrix, with significant changes in the transmittance value for wavelengths below 450 nm, especially for CS-PS20 film, compared to the control CS-C film. The transmittance at 700 nm was recorded as 90.9% for CS-C film, while the recorded values for CS-PS5, CS-PS10 and CS-PS20 films were 86.6%, 84.1% and 61.8%, respectively. The increase of PS concentration in the composite films showed a correlation with the decrease in their light transmission rate. A similar trend was observed in previous studies, reporting that the incorporation of extracts or essential oils to the CS film matrix causes a decrease in the film light transmittance rate together with increasing the film thickness [11–13,30].

Colour parameters including L^*, a^*, b^*, and ΔE^* values of CS-C and

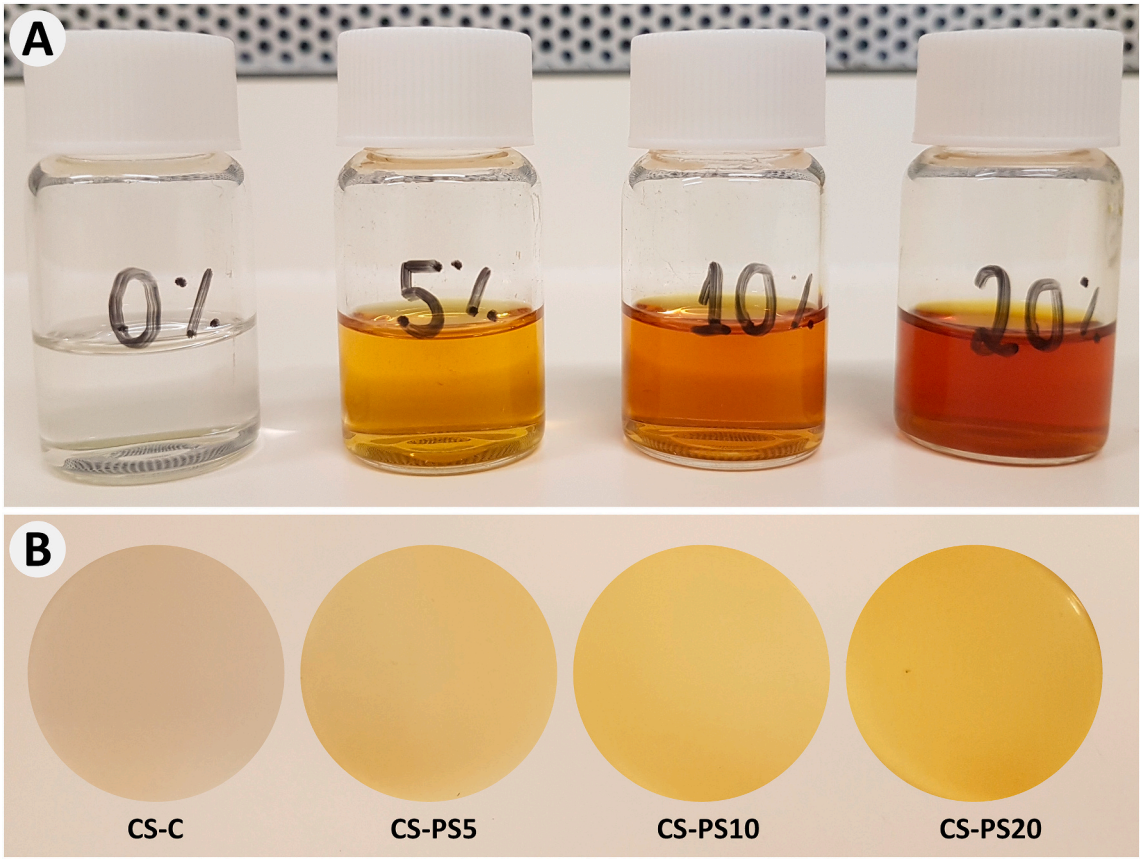

Fig. 2. A) Hydro-ethanolic PS extracts at different concentrations and B) the visual appearance of CS-C film and the CS-PS composite films with incorporated PS extract.

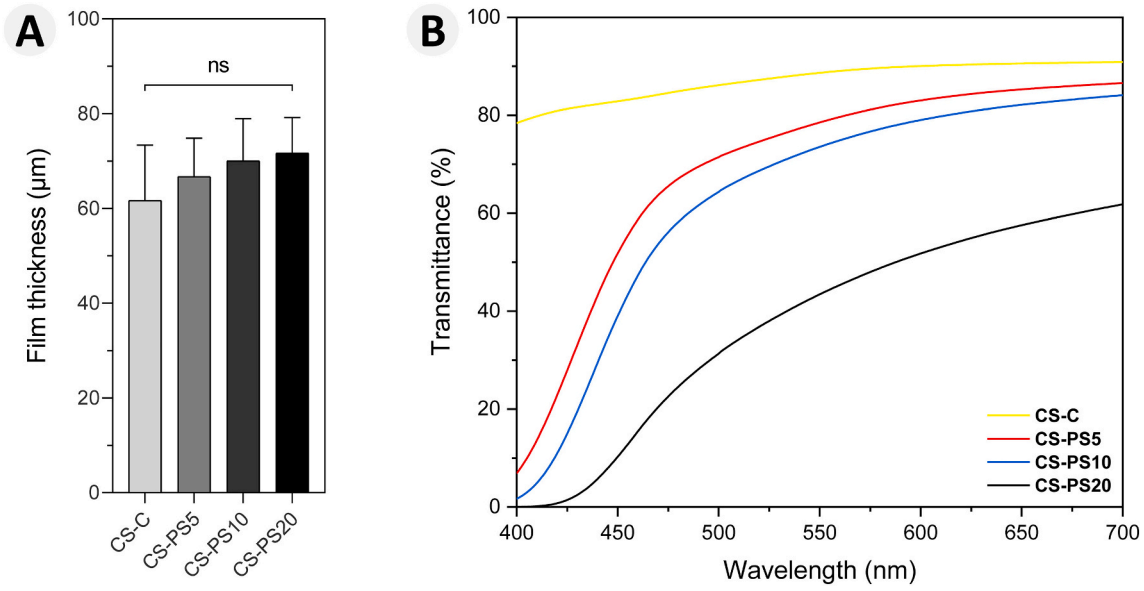

Fig. 3. A) Thickness and B) light transmittance of the CS-C film and the CS-PS composite films. ns: not significant.

CS-PS composite films are given in Table 1. For the CS-C film, a value of 88.2 ± 0.7 was measured for the lightness, L^*. A decrease of the L^* value was observed in parallel with the increasing addition of PS to the CS film matrix, with statistical significance ($p < 0.05$) among the results. With the exception of the CS-C film, the a^* parameter had slightly negative values indicating that the CS-PS composite films shifted towards a greenish colour without significant difference among them. The results also demonstrated that there were larger differences among the b^* values of the films compared to the other colour parameters, which increased depending on the amount of PS extract added to the film matrix. The colour difference, represented as ΔE^*, was calculated as 82.6 ± 0.6 for the CS-C film. This value increased with the percentage of

Table 1
L^*, a^*, b^* and ΔE^* parameters for the colour of the produced films.

Film	L^*	a^*	b^*	ΔE^*
CS-C	88.2 ± 0.7^{a}	0.5 ± 0.1^{a}	12.3 ± 0.1^{d}	82.6 ± 0.7^{c}
CS-PS5	85.6 ± 1.0^{b}	-1.6 ± 0.5^{b}	33.2 ± 2.7^{c}	85.0 ± 1.2^{b}
CS-PS10	84.6 ± 1.1^{bc}	-1.8 ± 1.0^{b}	39.6 ± 3.0^{b}	86.6 ± 0.6^{b}
CS-PS20	82.3 ± 1.0^{c}	-2.5 ± 0.7^{b}	51.0 ± 2.1^{a}	90.1 ± 1.0^{a}

Values are given as mean ± SD (n = 3). Different letters in the same column show significant differences ($p < 0.05$).

PS in the film and reached 90.1 ± 0.6 at the highest concentration (20%), which is a similar trend to that reported by Yang et al. [42] with the addition of 1.0% syringic acid, causing an increase in ΔE* value from 18.6 to 36.5. The behaviour in the colour parameters, and particularly a^* and b^* showed that the colour of the films with PS move towards greenish-yellowish tones, whereas the L^* value confirmed that the films becomes darker. This could be attributed to the pigments present in the chemical composition of PS and is consistent with other reported results of films from different biopolymers containing PS extract [16,23,43].

3.4. Structural properties

The FTIR spectra of CS, PS extract and films are presented in Fig. 4. In the CS, the peaks at 3356 and 2878 cm^{-1} were related to the –OH bonds and aliphatic C—H stretching vibration of CS [11]. The peaks at 1651, 1558, 1373 and 1026 cm^{-1} were attributed to C═O stretching (amide I), N—H bending (amide II), C—N stretching (amide III), and C—O stretching of alcohol groups, respectively [11]. In the PS extract, the band detected at 3271 cm^{-1} was due to the –OH groups of the phenolic compounds of PS or moisture, while bands at 2916 cm^{-1} and 2854 cm^{-1} were due to the asymmetric and symmetric stretching of CH_2, respectively [44]. Besides, the peak found at 1682 cm^{-1} in PS extract was attributed to C═O stretching of flavonoids, at 1605 cm^{-1} and 1512 cm^{-1} to aromatic ring deformations and at 1258 cm^{-1} to the vibration of C—O group of polyols, e.g., hydroxyflavonoids [45,46].

The FTIR spectra of the CS-PS5, CS-PS10 and CS-PS20 composite films showed a similar pattern to the spectra of the CS-C film, with slight changes at wavelengths of certain peaks and in their transmittance densities. The peak of 3263 cm^{-1} attributed to –OH stretching was similar to CS-C, CS-PS5 and CS-PS10 films, while it is shifted to 3271 cm^{-1} in CS-PS20 film with increasing PS concentration. The peaks at 2924 cm^{-1} and 2878 cm^{-1} exhibited stronger peak intensities in the PS containing films compared to the control film likely owing to stretching vibrations of the C—H bond in $–CH_2$ and $–CH_3$ groups of PS [16]. The peak of 1643 cm^{-1}, belonging to C═O, was similar for CS-C film and CS-PS5 but shifted to 1636 cm^{-1} in films with 10% and 20% of PS. This may be due to the effects of the benzene ring of the PS extract on the CS film matrix [45]. Along with this, there was no change in wavenumbers in the amide II band for all films, except for the transmittance densities. In the amide III band, responsible for C—N stretching, the CS-PS5, CS-PS10 and CS-PS20 films shifted to a higher wavelength and presented a more distinguishable shape with the increasing of PS concentration, while no significant peak was observed in the CS-C film. The absorption shifting to higher wavelengths could be explained by the resulting conjugation from the formation of covalent bonds between the reactive groups of CS and the aromatic ring of phenolic compounds in PS [47]. The covalent and hydrogen bonding between CS and PS occupy the functional groups of CS, thereby reducing the free hydrogen group which can form hydrophilic bonding with water, thus reflecting on the mechanical and barrier properties of the films [16]. According to the obtained results from FTIR, the shifting or broadening of some absorption bands reveals the existence of intermolecular interaction between the OH and NH_2 groups in CS and the phenolic compounds in PS extract, in agreement with previously reported studies [16,47,48], confirming the above mentioned changes on the film crosslinks, that influence the film thickness.

The degree of acetylation (DD) may vary for different CS sources which may affect its properties [49]. In our study the DD for the CS obtained from crayfish shells was calculated as 29%, which is lower than for *Metapenaeus stebbingi* (92.2%) [50] and *Rhinolophus hipposideros* guano (61%) [39], but higher than the value reported for *Euphausia superba* (11.3%) [40] and *Dociostaurus maroccanus* (22%) [51].

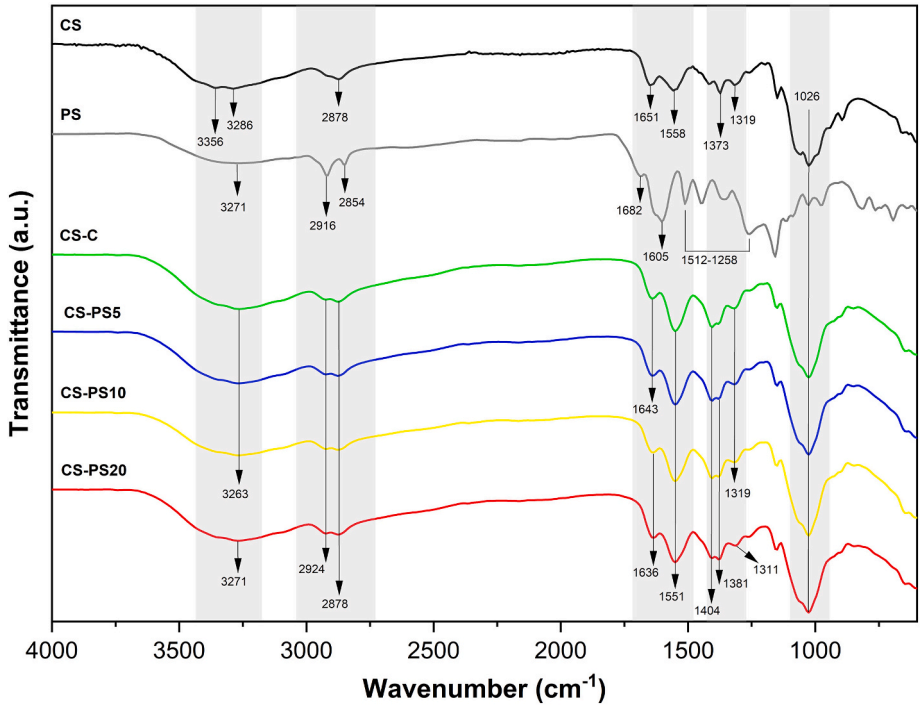

Fig. 4. FT-IR spectra of pure CS, PS extract, CS-C film and the CS-PS composite films.

3.5. Thermal properties

The results of TG/DTG analyses of CS, PS, and films are given in Fig. 5. As visualized in the figure, the mass loss for CS and PS occurred in two stages. The first loss between 30 and 100 °C (CS: 10.1% and PS: 1.1%) was due to the evaporation of water and ethanol in their structures. The second mass loss of 46.0% and 66.9%, occurring between 100 and 700 °C, was attributed to the decomposition of their structure, with the maximum degradation recorded at 303.7 °C for CS and 336.0 °C for PS [11,44]. In the case of the films, the mass loss occurred in three stages: i) around 8.9% at 30–100 °C, due to the evaporation of water in the polymeric structures; ii) an average of 11.4% at 120–220 °C, corresponding to the decomposition of low molecular weight compounds of the PS and glycerol and; iii) the main mass loss at 230–300 °C, attributed to the denaturation of CS polymeric structure and PS extract [11]. After the applied maximum temperature, the remaining ash content was recorded as 34.0% for CS, 28.4% for PS, and an average of 30% for the films.

The thermal stability of the composite films increased with the concentration of PS extract which could be the result of the higher degradation temperature of PS compared to CS, as demonstrated in Fig. 5, and the interactions between PS and the CS matrix. Since the thermal stability of the films is also related to the crystal structure [42], increasing PS concentration may have resulted in higher crystallinity and consequently more energy was needed to destroy the crystalline structure. Similarly, the reported TGA results for CS-banana peels extract [30] and CS-*Nigella sativa* seedcake extract [52] composite films was emphasized that thermal stability demonstrated an increasing trend with the addition of extracts to the film matrix. Besides, the current findings are in agreement with those reported by other authors for the thermal properties of films produced by adding different plant extracts and oils to the CS film matrix [11,53].

3.6. Microstructure of films

The surface characteristics of CS-C film, CS-PS5, CS-PS10 and CS-PS20 composite films are presented in Fig. 6. The surface morphology of the control film (Fig. 6A) were almost identical when compared to the CS-PS5 and CS-PS10 films (Fig. 6B and C). In the case of CS-PS20 (Fig. 6D), some homogeneously distributed greyish spots were observed in the film. A similar situation was noted for the starch and gelatine-based film containing PS extract reported previously [54,55]. The SEM images also reveal that the addition of up to 20% of PS to the CS film matrix did not cause significant modification of the film surface. The surface of all the films was generally smooth, compact and without any cracks or pores, suggesting good structural integrity by its compact and homogeneous structure.

3.7. Mechanical properties

The mechanical behaviour of the films was also investigated in order to observe the variations derived from the PS addition to the films, Fig. 7. For all the investigated parameters, there is a statistically significant ($p < 0.05$) difference between CS-C film and at least one of the films containing PS. Tensile modulus, defined as a measurement of the stiffness of a material, was 1638.9 ± 100.0 MPa for the CS-C film, Fig. 7A, while it enhanced by 20.7% (CS-PS5), 35.8% (CS-PS10) and 48.4% (CS-PS20) with increasing the concentration of PS. Significant improvements also occurred in yield strength and stress at break for all films containing PS extract. The CS-PS5 and CS-PS10 films had an improvement of 15.2% and 17.2% in their yield strength, respectively, however, a significant increase occurred for CS-PS20 with a value of 47.6%, Fig. 7B. A similar tendency was observed in the stress at break parameters, Fig. 7C. The intermolecular interactions between the components of the extracts and the CS polymer can lead to changes in mechanical characteristics of composite films such as stiffness, stress at break, and deformation [9,11,16,56]. Regarding the composite films in this study, it can be ascribed that the interactions between the hydrophilic groups of CS and the polyphenolic compounds of PS with polar properties resulted in the tightened polymer chain-chain interactions leading to stronger interfacial adhesion and higher resistance to mechanical stress [16]. As discussed in Section 3.4, the most significant changes between CS and PS occurred in the film with the highest concentration of PS, which seems to be reflected in its mechanical

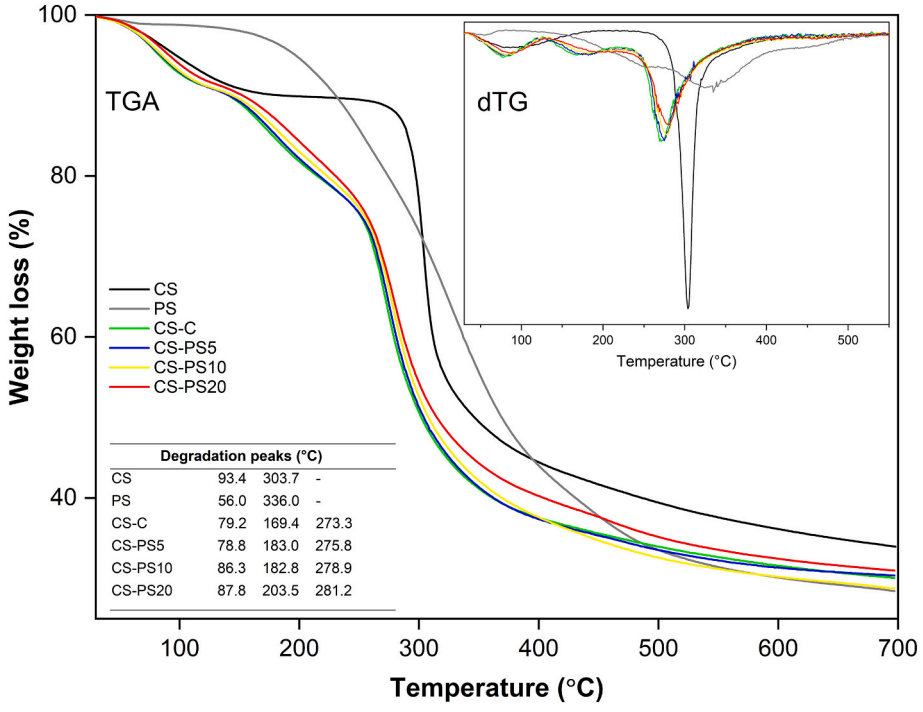

Fig. 5. TGA and DTG thermograms of pure CS, PS extract, CS-C film and the CS-PS composite films.

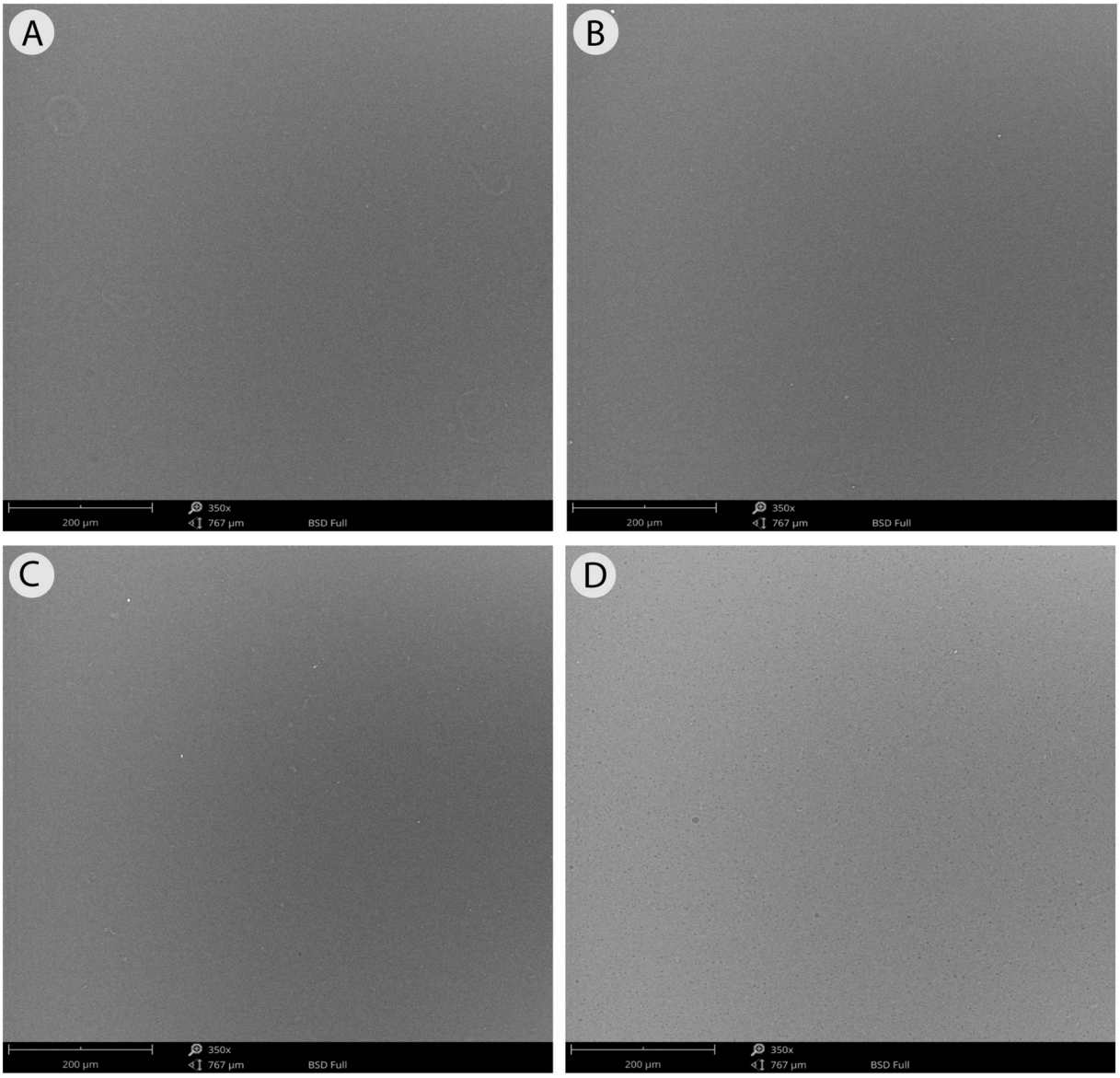

Fig. 6. Scanning electron microscopy of the CS-based films: A) CS-C film; B) CS-PS5 film; C) CS-PS10 film; and D) CS-PS20 film.

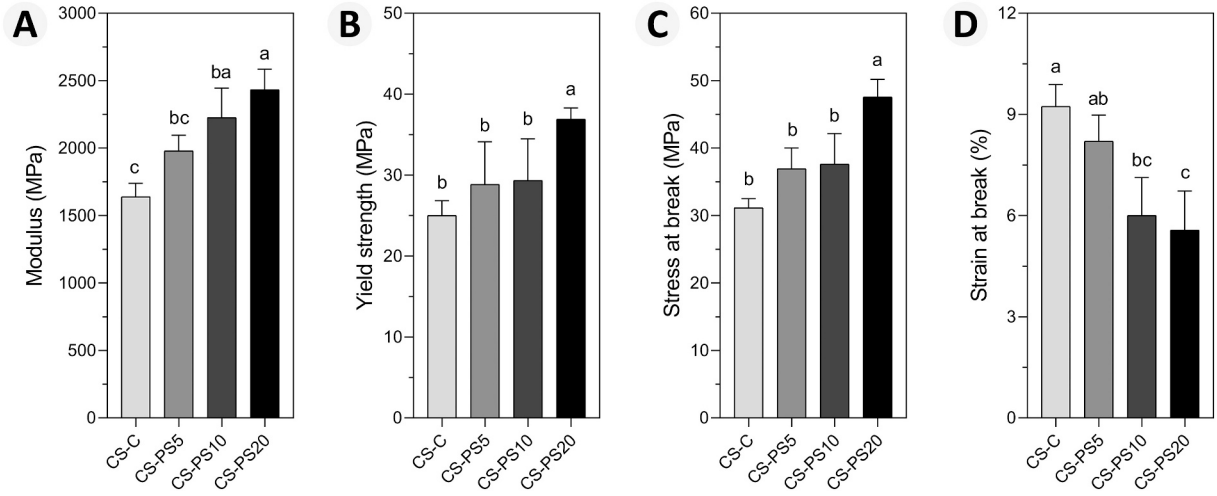

Fig. 7. Mechanical properties of CS-C film and the CS-PS composite films: A) modulus; B) yield strength; C) stress at break; and D) strain at break.

properties. Improvement in the mechanical properties of blend films with bioactive compounds was reported previously for biopolymeric films such as CS–green tea extract [56], CS–oak/hop extracts [9] and CS–terebinth extract [11].

On the other hand, the strain at break values of the films decreased with increasing PS concentration, Fig. 7D. That value for CS-C film was 9.2%, whereas for CS-PS5, CS-PS10 and CS-PS20 it was 8.2%, 6.0%, 5.6%, respectively. Although without statistical difference between CS-C film and CS-PS5, there was a significant difference when compared with CS-PS10 and CS-PS20. The addition of PS to the film matrix made the films stiffer, resulting in a reduction in the strain at break values of films and thus showed less elongation capacity. These results are consistent with those in the literature [16,22,57].

3.8. Degradation properties of films

The water solubility of biopolymer-based films is an important property in packaging since the film must maintain the necessary stability of the packaged food throughout its shelf life. In general, the structure of films with poor water resistance may soften when exposed to high humidity, and thus the molecules can pass through the film more easily as a result of changes in the film structure [58]. The water solubility rate was recorded as 45.7% for the CS-C film, Fig. 8A. This was lower than the value (58.0%) reported by Akyuz et al. [53], but it was higher than the result (24.0%) of Kaya et al. [11]. With the addition of PS to the CS film matrix, the water solubility of the composite films decreased significantly ($p < 0.05$), what could be related to strong intermolecular interactions between CS and bioactive compounds of PS extract [12], but also to the lower hydrophilicity of the PS components.

Regarding the degradation of composite films in soil, after 15 days, the films were completely degraded due to the enzymes produced by the microorganisms in the soil [53]. Besides, the diffusion of water into the polymer matrix may cause swelling and increase the biodegradation capacity of the films. The addition of PS to the films did not alter the soil degradation properties, so, the CS-PS composite films can be considered as rapidly degrading materials in nature, which strengthens the inferences of Akyuz et al. [53], who concluded that CS-based films produced by blending animal fat and plant oil degraded at high rates under soil incubation.

3.9. Biological properties

3.9.1. Antioxidant activity

The free radical scavenging capacities of the films are presented in Fig. 8B and C. It is known that CS has some intrinsic antioxidant activity due to the formation of stable molecules as a consequence of the reaction of free radicals with its amino groups [16]. In this study, the radical scavenging activity of the CS-C film was recorded as 2.5% and 4.9% for DPPH and ABTS, respectively, confirming that the control film was not a strong scavenger for DPPH and ABTS radicals.

The addition of PS extract resulted in a significant improvement ($p < 0.05$) in the antioxidant activity of films. DPPH radical scavenging capacity increased up to 49.8%, 94.0% and 94.5% for CS-PS5, CS-PS10 and CS-PS20 films, respectively, while it was recorded as 20.3%, 54.6% and 83.6% for ABTS. The antioxidant activity of the active films containing the highest concentration of PS increased approximately 38 times for DPPH and more than 17 times for ABTS compared to the control film. This effect could be attributed to activity of phenolic compounds coming from the PS extract [17]. These findings are consistent with previously reported antioxidant results of active polymeric films containing PS [55,59]. The better performance towards DPPH compared to the ABTS assay could be explained by the difference interaction mechanisms between the phenolic compounds of PS and the ABTS/DPPH radicals: the ABTS test can be applied to both hydrophilic and hydrophobic antioxidant systems, while the DPPH test it only applicable to hydrophobic systems [60] since it employs a radical dissolved in an organic medium, hence it may favour the interactions with the hydrophobic phenolic compounds of PS, particularly the flavonoids. The releasing time is another factor that may condition the antioxidant capacity of the active films and the fate of the solution which is used for antioxidant analysis [61]. Some authors highlighted that the antioxidant properties of CS films blended with protocatechuic acid could vary significantly according to the release time [57]. In the study, while the DPPH radical scavenging activity of the composite film taken in the first hour was around 5%, this activity increased to over 90% after 24 h.

3.9.2. Antimicrobial assays

PS extract is a natural antimicrobial agent against human and foodborne pathogenic microorganisms, so, its incorporation on package films is a creative mechanism to avoid or reduce the growth of bacteria, yeast and moulds on the packaged materials. To evaluate the

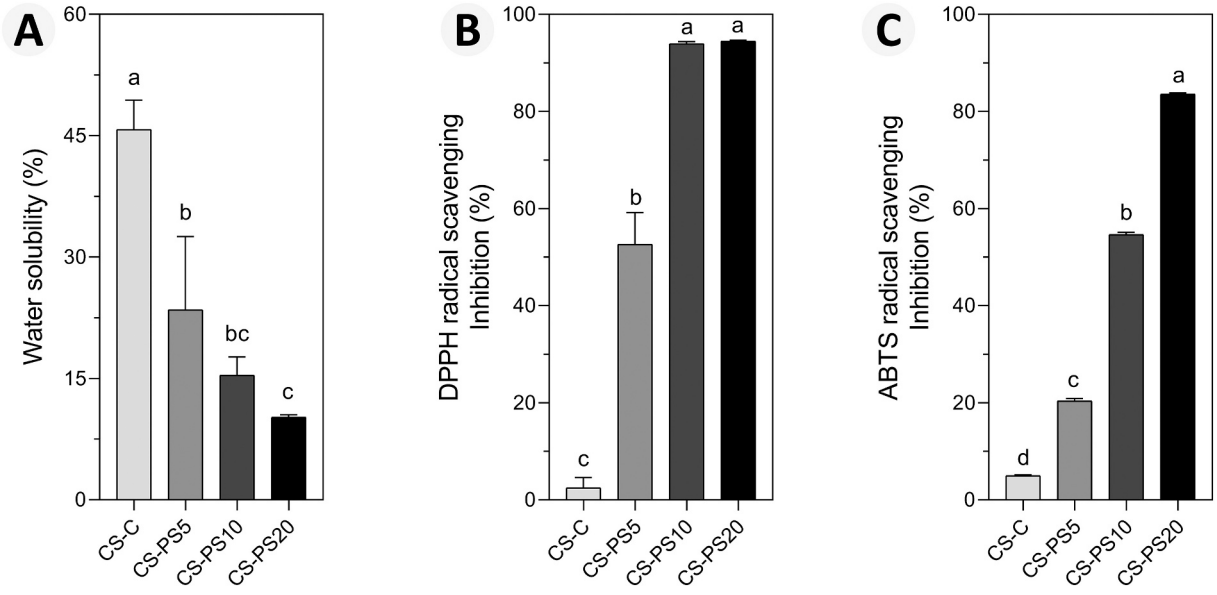

Fig. 8. Water solubility and antioxidant capacities of CS-C film and the CS-PS composite films: A) water solubility; B) DPPH free radical scavenging activity; and C) ABTS free radical scavenging activity.

performance of the films, they were compared with antifungal and antibacterial agents (Teldor® and ampicillin sodium salt) and a control solution (mixture of glycerol, ethanol, and acetic acid), Fig. 9.

According to the results, no inhibition zone was observed for the control group and CS-C film, for all microorganisms, Fig. 9A and B. Nevertheless, in most cases, there was no microbial growth in the area where the CS-C film was in contact with the medium and its upper part, Fig. 9C and D. This could be attributed to the inherent antimicrobial characteristic of CS [11]. The CS-PS5 film was effective against *Arthrobacter* sp. and *M. rancensis* with inhibition zone values of 1.1 ± 0.2 mm and 1.0 ± 0.1 mm, respectively. For the CS-PS10 film, in addition to *Arthrobacter* sp. (1.6 ± 0.3 mm) and *M. rancensis* (1.7 ± 0.2 mm), it also showed an inhibitory effect against *S. aureus* with an inhibition hallo of 2.8 ± 0.1 mm. CS-PS20 film exhibited higher antimicrobial activity compared to all the other films, with inhibition zone values of 3.8 ± 0.3 mm, 1.9 ± 0.5 mm and 1.0 ± 0.03 mm against *Arthrobacter* sp., *S. aureus*, and *S. hominis*, respectively, all gram-positive bacteria. Similarly, the CS-PS20 film was also effective against the mould *M. rancensis* with a value of 1.88 ± 0.2 mm.

The antimicrobial activity of the films on the tested microorganisms was in most cases, limited to the area of physical contact only. Even though several studies reported that CS-based films containing different kinds of plant extracts and oils were effective by forming inhibition areas against human and foodborne pathogenic microorganisms [9,11,53], the tested composite films demonstrated no inhibition zones, especially against gram-negative bacteria and fungi. Torlak and Sert [62] stated that CS-based films did not show antimicrobial activity by agar diffusion, because the chitosan in the film form could not pass through the adjacent agar media. In a similar study, Siripatrawan et al. [16] performed the antimicrobial activity of CS composite films using the disc diffusion method and reported that microbial growth was inhibited only in the area where the discs were in direct contact with the medium. Another possible mechanism to elucidate the antimicrobial activity of composite films can be explained by the chemical effects of caffeic acid, quercetin, chrysin, pinobanksin, galangin and similar phenolic compounds released from the films. As visualized in Fig. 9C, inhibition zones could be seen around films, which could be characterized as a chemical effect caused by the phenolic compounds in PS, as well as the areas of direct physical contact of the films with the media. This situation could be more clearly distinguished by the increase in the concentration of the PS extract.

Overall, it could be concluded that CS film matrix did not have a high diffusion ability in the adjacent agar medium and did not exhibit notable antimicrobial activity around the applied area due to the absence of possible interactions between polymer chains and/or phenolic compounds and pathogen cell walls [62,63]. However, it has to be highlighted, in direct physical contact, the CS films enriched with PS are effective to all gram-positive, gram-negative, mould, and fungi evaluated. In food packaging or coating processes, this feature may be considered reasonable for such processes, since the entire food is surrounded by the film.

4. Conclusions

This work demonstrated that biodegradable films for food packaging could be produced by incorporating CS obtained from the waste shells of crayfish with PS extracts, which has been explored in the food industry as a natural source of antimicrobial and antioxidant agents. The obtained data indicated that adding PS to the CS film matrix could result in a remarkable improvement in both, the physicochemical and biological properties of the films, hence showing that PS is a suitable additive. Besides, with the increase of PS ratio in the film matrix, the functionality

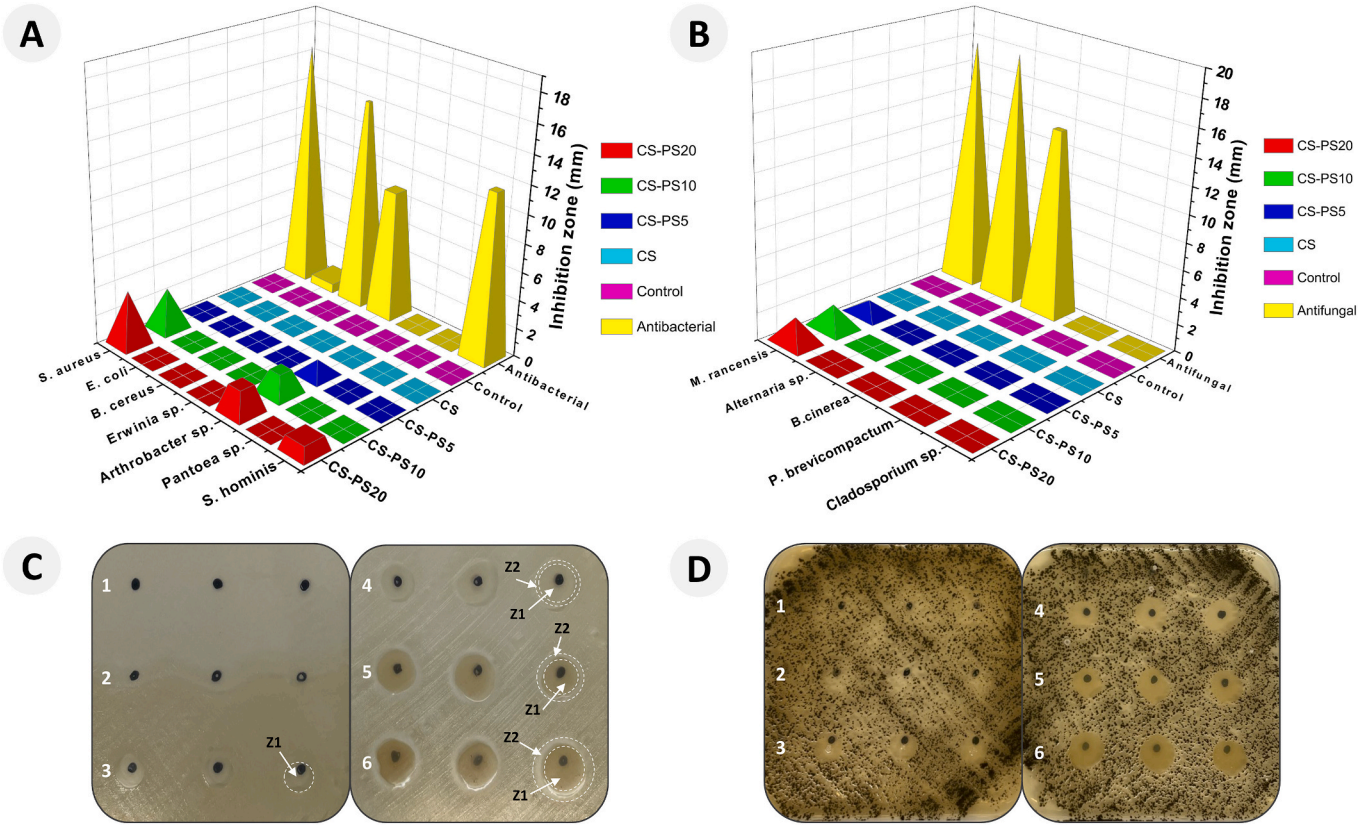

Fig. 9. Inhibition zone of CS-C film and CS-PS composite films against bacteria (A) and fungi (B) by the agar drop diffusion test. Example of antimicrobial activity of the films against *Staphylococcus aureus* (C) and *Cladosporium* sp. (D). In the Petri dishes: row 1 = antifungal agent, row 2 = the control group, row 3 = CS-C film, row 4 = CS-PS5 film, row 5 = CS-PS10 film and row 6 = CS-PS20 film (three repetitions). Z1: zone of direct physical contact; Z2: zone of chemical effect/diffusion.

of active packaging films increases in most cases. The current data suggest the possibility of using CS-PS composite films as a green and eco-friendly approach for packaging oxidation-sensitive food products and increasing their shelf life replacing petroleum-based synthetic plastics that are not biodegradable.

CRediT authorship contribution statement

Conceptualization, V. Aylanc, C. Pereira, P. Rodrigues, M. Vilas-Boas, S.I. Falcão; Methodology and data analysis C. De Carli, V. Aylanc, K.M. Mouffok, A. Tomás, P. Rodrigues; writing—original draft preparation, C. De Carli, V. Aylanc, S.I. Falcão; writing—review and editing, A. Santamaria-Echart, F. Barreiro, C. Pereira, P. Rodrigues, M. Vilas-Boas, S.I. Falcão; supervision, A. Santamaria-Echart, S.I. Falcão; funding acquisition, F. Barreiro, M. Vilas-Boas. All authors have read and agreed to the published version of the manuscript.

Declaration of competing interest

The authors declare no conflict of interest.

Acknowledgments

The authors are grateful to the Foundation for Science and Technology (FCT, Portugal) for financial support by national funds FCT/MCTES to CIMO (UIDB/00690/2020) and contracts through the individual and institutional scientific employment program-contract with Soraia I. Falcão and Arantzazu Santamaria Echart. Thanks to the Programa Apícola Nacional 2020-2022 (National Beekeeping Program) for funding the project “Standardization of production procedures and quality parameters of bee products” and to Project PDR2020-1.0.1-FEADER-031734: “DivInA-Diversification and Innovation on Beekeeping Production”. Finally, this work is funded by the European Regional Development Fund (ERDF) through the Regional Operational Program North 2020, within the scope of Project GreenHealth - Digital strategies in biological assets to improve well-being and promote green health, Norte-01-0145-FEDER-000042.

Appendix A. Supplementary data

Supplementary data to this article can be found online at https://doi.org/10.1016/j.ijbiomac.2022.05.155.

References

[1] A. Mittal, A. Singh, S. Benjakul, T. Prodpran, K. Nilsuwan, N. Huda, K. de la Caba, Composite films based on chitosan and epigallocatechin gallate grafted chitosan: characterization, antioxidant and antimicrobial activities, Food Hydrocoll. 111 (2021), 106384.
[2] F. Bigi, H. Haghighi, H.W. Siesler, F. Licciardello, A. Pulvirenti, Characterization of chitosan-hydroxypropyl methylcellulose blend films enriched with nettle or sage leaf extract for active food packaging applications, Food Hydrocoll. 120 (2021), 106979.
[3] N.L. vanden Braber, L. di Giorgio, C.A. Aminahuel, L.I.D. Vergara, A.O.M. Costa, M. A. Montenegro, A.N. Mauri, Antifungal whey protein films activated with low quantities of water soluble chitosan, Food Hydrocoll. 110 (2021), 106156.
[4] S. Roy, J.-W. Rhim, Preparation of gelatin/carrageenan-based color-indicator film integrated with shikonin and propolis for smart food packaging applications, ACS Appl. Bio Mater. 4 (2020) 770–779.
[5] M. Kaya, I. Sargin, V. Aylanc, M.N. Tomruk, S. Gevrek, I. Karatoprak, N. Colak, Y. G. Sak, E. Bulut, Comparison of bovine serum albumin adsorption capacities of α-chitin isolated from an insect and β-chitin from cuttlebone, J. Ind. Eng. Chem. 38 (2016) 146–156.
[6] H. Yong, J. Liu, Active packaging films and edible coatings based on polyphenol-rich propolis extract: a review, Compr. Rev. Food Sci. Food Saf. 20 (2021) 2106–2145.
[7] I. Aranaz, N. Acosta, C. Civera, B. Elorza, J. Mingo, C. Castro, A.Heras Caballero, M. D. los L. Gandía, Cosmetics and cosmeceutical applications of chitin, chitosan and their derivatives, Polymers 10 (2018) 213.
[8] A. Moeini, P. Pedram, P. Makvandi, M. Malinconico, G.G. d'Ayala, Wound healing and antimicrobial effect of active secondary metabolites in chitosan-based wound dressings: a review, Carbohydr. Polym. 233 (2020), 115839.
[9] M. Bajić, T. Ročnik, A. Oberlintner, F. Scognamiglio, U. Novak, B. Likozar, Natural plant extracts as active components in chitosan-based films: a comparative study, Food Packag. Shelf Life 21 (2019), 100365.
[10] R. Fernández-Marín, S.C.M. Fernandes, M.Á.A. Sánchez, J. Labidi, Halochromic and antioxidant capacity of smart films of chitosan/chitin nanocrystals with curcuma oil and anthocyanins, Food Hydrocoll. 123 (2021), 107119.
[11] M. Kaya, S. Khadem, Y.S. Cakmak, M. Mujtaba, S. Ilk, L. Akyuz, A.M. Salaberria, J. Labidi, A.H. Abdulqadir, E. Deligöz, Antioxidative and antimicrobial edible chitosan films blended with stem, leaf and seed extracts of Pistacia terebinthus for active food packaging, RSC Adv. 8 (2018) 3941–3950.
[12] M. Kaya, P. Ravikumar, S. Ilk, M. Mujtaba, L. Akyuz, J. Labidi, A.M. Salaberria, Y. S. Cakmak, S.K. Erkul, Production and characterization of chitosan based edible films from Berberis crataegina's fruit extract and seed oil, Innov. Food Sci. Emerg. Technol. 45 (2018) 287–297.
[13] T. Liu, J. Wang, F. Chi, Z. Tan, L. Liu, Development and characterization of novel active chitosan films containing fennel and peppermint essential oils, Coatings. 10 (2020) 936.
[14] N. Zhang, F. Bi, F. Xu, H. Yong, Y. Bao, C. Jin, J. Liu, Structure and functional properties of active packaging films prepared by incorporating different flavonols into chitosan based matrix, Int. J. Biol. Macromol. 165 (2020) 625–634.
[15] Y. Zou, C. Zhang, P. Wang, Y. Zhang, H. Zhang, Electrospun chitosan/polycaprolactone nanofibers containing chlorogenic acid-loaded halloysite nanotube for active food packaging, Carbohydr. Polym. 247 (2020), 116711.
[16] U. Siripatrawan, W. Vitchayakitti, Improving functional properties of chitosan films as active food packaging by incorporating with propolis, Food Hydrocoll. 61 (2016) 695–702.
[17] S.I. Falcão, A. Tomás, N. Vale, P. Gomes, C. Freire, M. Vilas-Boas, Phenolic quantification and botanical origin of Portuguese propolis, Ind. Crop. Prod. 49 (2013) 805–812.
[18] T.D. Tran, S.M. Ogbourne, P.R. Brooks, N. Sánchez-Cruz, J.L. Medina-Franco, R. J. Quinn, Lessons from exploring chemical space and chemical diversity of propolis components, Int. J. Mol. Sci. 21 (2020) 4988.
[19] A. Salatino, C.C. Fernandes-Silva, A.A. Righi, M.L.F. Salatino, Propolis research and the chemistry of plant products, Nat. Prod. Rep. 28 (2011) 925–936.
[20] N. Aminimoghadamfarouj, A. Nematollahi, Propolis diterpenes as a remarkable bio-source for drug discovery development: a review, Int. J. Mol. Sci. 18 (2017) 1290.
[21] S.I. Falcão, R.C. Calhelha, S. Touzani, B. Lyoussi, I.C.F.R. Ferreira, M. Vilas-Boas, In vitro interactions of moroccan propolis phytochemical's on human tumor cell lines and anti-inflammatory properties, Biomolecules. 9 (2019) 315.
[22] S. Hajinezhad, B.M. Razavizadeh, R. Niazmand, I. Ghasemi, Antimicrobial, mechanical, and physicochemical properties of ethylene vinyl alcohol (EVOH) extruded films blended with propolis, Int. J. Food Prop. 23 (2020) 2020–2032.
[23] L.D. Pérez-Vergara, M.T. Cifuentes, A.P. Franco, C.E. Pérez-Cervera, R.D. Andrade-Pizarro, Development and characterization of edible films based on native cassava starch, beeswax, and propolis, NFS J. 21 (2020) 39–49.
[24] K. Skowron, J. Kwiecińska-Piróg, K. Grudlewska, G. Gryń, N. Wiktorczyk, M. Balcerek, D. Załuski, E. Wałecka-Zacharska, S. Kruszewski, E. Gospodarek-Komkowska, Antilisterial activity of polypropylene film coated with chitosan with propolis and/or bee pollen in food models, Biomed. Res. Int. 2019 (2019) 1–12.
[25] V. Aylanc, A. Tomás, P. Russo-Almeida, S.I. Falcão, M. Vilas-Boas, Assessment of bioactive compounds under simulated gastrointestinal digestion of bee pollen and bee bread: bioaccessibility and antioxidant activity, Antioxidants 10 (2021).
[26] F. Duman, M. Kaya, Crayfish chitosan for microencapsulation of coriander (Coriandrum sativum L.) essential oil, Int. J. Biol. Macromol. 92 (2016) 125–133.
[27] K. Halász, L. Csóka, Black chokeberry (Aronia melanocarpa) pomace extract immobilized in chitosan for colorimetric pH indicator film application, food packag. ShelfLife 16 (2018) 185–193.
[28] A. Baxter, M. Dillon, K.D.A. Taylor, G.A.F. Roberts, Improved method for ir determination of the degree of N-acetylation of chitosan, Int. J. Biol. Macromol. 14 (1992) 166–169.
[29] V. Aylanc, S. Ertosun, L. Akyuz, B.K. Bilican, S. Gokdag, I. Bilican, Y.S. Cakmak, B. A. Yilmaz, M. Kaya, Natural β-chitin-protein complex film obtained from waste razor shells for transdermal capsaicin carrier, Int. J. Biol. Macromol. 155 (2020) 508–515.
[30] W. Zhang, X. Li, W. Jiang, Development of antioxidant chitosan film with banana peels extract and its application as coating in maintaining the storage quality of apple, Int. J. Biol. Macromol. 154 (2020) 1205–1214.
[31] J. Gomes, J. Barbosa, P. Teixeira, The inhibitory concentration of natural food preservatives may be biased by the determination methods, Foods 10 (2021) 1009.
[32] S.I. Falcão, N. Vale, P. Gomes, M.R.M. Domingues, C. Freire, S.M. Cardoso, M. Vilas-Boas, Phenolic profiling of Portuguese propolis by LC–MS spectrometry: uncommon propolis rich in flavonoid glycosides, Phytochem. Anal. 24 (2013) 309–318.
[33] M. Woźniak, L. Mrówczyńska, A. Waśkiewicz, T. Rogoziński, I. Ratajczak, Phenolic profile and antioxidant activity of propolis extracts from Poland, Nat. Prod. Commun. 14 (2019).
[34] E.C.A. de Souza, E.J.G. da Silva, H.K.C. Cordeiro, N.M. Lage, F. Silva, D.L.S. dos Reis, C. Porto, E.J. Pilau, L.A. Costa, A.D.L. de Souza, Chemical compositions and antioxidant and antimicrobial activities of propolis produced by Frieseomelitta longipes and Apis mellifera bees, Quim Nova 41 (2018) 485–491.
[35] V. Aylanc, B. Eskin, G. Zengin, M. Dursun, Y.S. Cakmak, In vitro studies on different extracts of fenugreek (Trigonella spruneriana BOISS.): phytochemical profile, antioxidant activity, and enzyme inhibition potential, J. Food Biochem. 44 (2020), e13463.

[36] K. Pobiega, J.L. Przybył, J. Żubernik, M. Gniewosz, Prolonging the shelf life of cherry tomatoes by pullulan coating with ethanol extract of propolis during refrigerated storage, Food Bioprocess Technol. 13 (2020) 1447–1461.
[37] N.H. Marei, E.A. El-Samie, T. Salah, G.R. Saad, A.H.M. Elwahy, Isolation and characterization of chitosan from different local insects in Egypt, Int. J. Biol. Macromol. 82 (2016) 871–877.
[38] J. Ma, C. Xin, C. Tan, Preparation, physicochemical and pharmaceutical characterization of chitosan from Catharsius molossus residue, Int. J. Biol. Macromol. 80 (2015) 547–556.
[39] M. Kaya, O. Seyyar, T. Baran, T. Turkes, Bat guano as new and attractive chitin and chitosan source, Front. Zool. 11 (2014) 1–10.
[40] Y. Wang, Y. Chang, L. Yu, C. Zhang, X. Xu, Y. Xue, Z. Li, C. Xue, Crystalline structure and thermal property characterization of chitin from Antarctic krill (Euphausia superba), Carbohydr. Polym. 92 (2013) 90–97.
[41] E.S. Abdou, K.S.A. Nagy, M.Z. Elsabee, Extraction and characterization of chitin and chitosan from local sources, Bioresour. Technol. 99 (2008) 1359–1367.
[42] K. Yang, H. Dang, L. Liu, X. Hu, X. Li, Z. Ma, X. Wang, T. Ren, Effect of syringic acid incorporation on the physical, mechanical, structural and antibacterial properties of chitosan film for quail eggs preservation, Int. J. Biol. Macromol. 141 (2019) 876–884.
[43] C. Pastor, L. Sánchez-González, M. Cháfer, A. Chiralt, C. González-Martínez, Physical and antifungal properties of hydroxypropylmethylcellulose based films containing propolis as affected by moisture content, Carbohydr. Polym. 82 (2010) 1174–1183.
[44] S. Hajinezhad, B.M. Razavizadeh, R. Niazmand, Study of antimicrobial and physicochemical properties of LDPE/propolis extruded films, Polym. Bull. 77 (2020) 4335–4353.
[45] J.R. Franca, M.P. de Luca, T.G. Ribeiro, R.O. Castilho, A.N. Moreira, V.R. Santos, A. A.G. Faraco, Propolis-based chitosan varnish: drug delivery, controlled release and antimicrobial activity against oral pathogen bacteria, BMC Complement. Altern. Med. 14 (2014) 1–11.
[46] R.N. Oliveira, M.C. Mancini, F.C.S. de Oliveira, T.M. Passos, B. Quilty, R.M. da S.M. Thiré, G.B. McGuinness, FTIR analysis and quantification of phenols and flavonoids of five commercially available plants extracts used in wound healing, Matéria (Rio J.) 21 (2016) 767–779.
[47] M. Curcio, F. Puoci, F. Iemma, O.I. Parisi, G. Cirillo, U.G. Spizzirri, N. Picci, Covalent insertion of antioxidant molecules on chitosan by a free radical grafting procedure, J. Agric. Food Chem. 57 (2009) 5933–5938.
[48] Z.N. Correa-Pacheco, S. Bautista-Baños, M. de Lorena Ramos-García, M. del Carmen Martínez-González, J. Hernández-Romano, Physicochemical characterization and antimicrobial activity of edible propolis-chitosan nanoparticle films, Prog. Org. Coat. 137 (2019), 105326.
[49] M.E. Abd El-Hack, M.T. El-Saadony, M.E. Shafi, N.M. Zabermawi, M. Arif, G. E. Batiha, A.F. Khafaga, Y.M. Abd El-Hakim, A.A. Al-Sagheer, Antimicrobial and antioxidant properties of chitosan and its derivatives and their applications: a review, Int. J. Biol. Macromol. 164 (2020) 2726–2744.
[50] A. Kucukgulmez, M. Celik, Y. Yanar, D. Sen, H. Polat, A.E. Kadak, Physicochemical characterization of chitosan extracted from Metapenaeus stebbingi shells, Food Chem. 126 (2011) 1144–1148.
[51] S. Erdogan, M. Kaya, High similarity in physicochemical properties of chitin and chitosan from nymphs and adults of a grasshopper, Int. J. Biol. Macromol. 89 (2016) 118–126.
[52] D. Kadam, N. Shah, S. Palamthodi, S.S. Lele, An investigation on the effect of polyphenolic extracts of Nigella sativa seedcake on physicochemical properties of chitosan-based films, Carbohydr. Polym. 192 (2018) 347–355.
[53] L. Akyuz, M. Kaya, S. Ilk, Y.S. Cakmak, A.M. Salaberria, J. Labidi, B.A. Yılmaz, I. Sargin, Effect of different animal fat and plant oil additives on physicochemical, mechanical, antimicrobial and antioxidant properties of chitosan films, Int. J. Biol. Macromol. 111 (2018) 475–484.
[54] R.B. Bodini, P.J.D.A. Sobral, C.S. Favaro-Trindade, R.A. Carvalho, Properties of gelatin-based films with added ethanol–propolis extract, LWT - Food Sci. Technol. 51 (2013) 104–110.
[55] G.K.P. de Araújo, S.J. de Souza, M.V. da Silva, F. Yamashita, O.H. Gonçalves, F. V. Leimann, M.A. Shirai, Physical, antimicrobial and antioxidant properties of starch-based film containing ethanolic propolis extract, Int. J. Food Sci. Technol. 50 (2015) 2080–2087.
[56] U. Siripatrawan, B.R. Harte, Physical properties and antioxidant activity of an active film from chitosan incorporated with green tea extract, Food Hydrocoll. 24 (2010) 770–775.
[57] J. Liu, S. Liu, Q. Wu, Y. Gu, J. Kan, C. Jin, Effect of protocatechuic acid incorporation on the physical, mechanical, structural and antioxidant properties of chitosan film, Food Hydrocoll. 73 (2017) 90–100.
[58] X. Chang, Y. Hou, Q. Liu, Z. Hu, Q. Xie, Y. Shan, G. Li, S. Ding, Physicochemical and antimicrobial properties of chitosan composite films incorporated with glycerol monolaurate and nano-TiO2, Food Hydrocoll. 119 (2021), 106846.
[59] P.A. Ulloa, J. Vidal, C. Lopéz de Dicastillo, F. Rodriguez, A. Guarda, R.M.S. Cruz, M.J. Galotto, Development of poly (lactic acid) films with propolis as a source of active compounds: biodegradability, physical, and functional properties, J. Appl. Polym. Sci. 136 (2019) 47090.
[60] A. Floegel, D.-O. Kim, S.-J. Chung, S.I. Koo, O.K. Chun, Comparison of ABTS/DPPH assays to measure antioxidant capacity in popular antioxidant-rich US foods, J. Food Compos. Anal. 24 (2011) 1043–1048.
[61] M. Moradi, H. Tajik, S.M. Razavi Rohani, A.R. Oromiehie, H. Malekinejad, J. Aliakbarlu, M. Hadian, Characterization of antioxidant chitosan film incorporated with Zataria multiflora Boiss essential oil and grape seed extract, LWT - Food Sci. Technol. 46 (2012) 477–484.
[62] E. Torlak, D. Sert, Antibacterial effectiveness of chitosan–propolis coated polypropylene films against foodborne pathogens, Int. J. Biol. Macromol. 60 (2013) 52–55.
[63] P. Fernandez-Saiz, J.M. Lagaron, P. Hernandez-Muñoz, M.J. Ocio, Characterization of antimicrobial properties on the growth of S. aureus of novel renewable blends of gliadins and chitosan of interest in food packaging and coating applications, Int. J. Food Microbiol. 124 (2008) 13–20.